

# $m_b$ from ALEPH and comparison with other LEP experiments.

Fabrizio Palla<sup>a</sup> \*

<sup>a</sup>CERN, CH-1211 Geneva 23, Switzerland

I will review the measurements of the  $b$ -quark mass performed by ALEPH and DELPHI. A large set of observables has been used together with detailed studies on jet algorithms. Very clear effects due to the  $b$ -quark mass running are observed. Comparing with the determinations at the  $\Upsilon(4S)$  threshold, the measurements of the running  $b$ -quark mass at the  $Z$  pole are consistent with the predicted evolution from QCD.

## 1. Introduction

The  $b$ -quark mass is one of the fundamental parameters of the QCD Lagrangian. However, due to confinement, quarks do not appear as free particles and therefore the definition of their mass is ambiguous. In fact, quark masses can either be defined as for free particles (such as the leptons) as the position of the pole of the propagator, or they can be interpreted as effective coupling constants in the Lagrangian. In the former definition the mass is called “pole mass” and does not run with energy; in the latter the mass is called “running mass”; as such it is a scale and renormalization scheme dependent quantity.

The  $b$ -quark mass is important for phenomenology since it enters many theoretical predictions of physical quantities such as CKM matrix elements,  $b$ -hadron inclusive semileptonic decays, total widths.

Most of the  $b$ -quark mass determinations have been extracted at the  $\Upsilon(4S)$  threshold, from the  $\Upsilon$  bound states with QCD sum rules [1] and QCD lattice calculations[2]. It is therefore interesting to measure this parameter at higher scales such as the one offered by LEP.

At LEP, the possibility to test the running of the  $b$ -quark mass within the framework of the perturbative QCD had not been considered until very recently. The reason is that the effects of the mass rapidly become very small with increasing energy for many observables, since they are pro-

portional to  $m_b^2/M_Z^2$  ( $\mathcal{O}(0.1\%)$ ), for instance in the total cross section. For other quantities, such as jet rates, the effects are of the order of few percent due to the suppression of the radiation off  $b$  quarks. The advent of theoretical calculations at next-to-leading order (NLO) in QCD perturbation theory allowed for the determination of the  $b$ -quark mass [3].

In this article I will review the measurements done by ALEPH[4] using a large set of event shape observables and by DELPHI[5,6] using the three-jet rate. The different sensitivity to the hadronization corrections and next-to-leading order corrections can be used to investigate the interpretation of the results.

## 2. Analysis Method

The method to extract the  $b$ -quark mass is based on measuring the ratio of any infrared safe observable  $O$  computed for  $b$  and  $uds$  (referred as  $q$ ) induced events and assuming  $\alpha_s$  universality,

$$R_{bq}^{pert} = O_b/O_q. \quad (1)$$

The following variables have been studied by ALEPH:

- The rate of three-jet events, where jets are reconstructed using the DURHAM [7] clustering algorithm with  $y_{cut} = 0.02$ .
- The first and the second moments of the event shape variables Thrust  $T$ , C-parameter  $C$ ,  $y_3$ , Total and Wide Jet Broadening,  $B_T$  and  $B_W$ . The definitions of the

\*On leave from Istituto Nazionale di Fisica Nucleare, Sezione di Pisa

observables can be found, e.g., in [8,9] and references therein.

DELPHI has used the three and the four jet event rates.

The measured ratio  $R_{bq}^{\text{meas}}$  of the observables in  $b$ -tagged events and in  $uds$ -tagged events can be related to the quantities at the parton level via the following formula

$$R_{bq}^{\text{meas}} = (O_b H_b D_b T_{bb} \mathcal{P}_{bb} + O_c H_c D_c T_{bc} \mathcal{P}_{bc} + O_q H_q D_q T_{bq} \mathcal{P}_{bq}) / (O_b H_b D_b T_{qb} \mathcal{P}_{qb} + O_c H_c D_c T_{qc} \mathcal{P}_{qc} + O_q H_q D_l T_{qq} \mathcal{P}_{qq}). \quad (2)$$

Here  $H_x, D_x, T_{yx}$  are the corrections due to hadronization, detector effects and tagging, respectively, and  $\mathcal{P}_{yx}$  are the purities of the tagged sample, where  $x$  is the true flavour and  $y$  is the tagged one. The tagging corrections take into account biases introduced by the flavour tag. In case of ALEPH the ratio is computed with respect to an unbiased sample of all flavours, which means that  $\mathcal{P}_{qx}$  is equal to the ratio of the partial width of the  $Z$  to  $x$  quarks and the total hadronic width, and  $T_{qx} = 1$ .

All the correction factors and purities are obtained from Monte Carlo (MC) simulations. Because mainly ratios of corrections are involved, some systematic uncertainties cancel.

$R_{bq}^{\text{pert}}$  is extracted from the relationship (2) and finally corrected for the contribution of anomalous triangle diagrams [10], in order to relate  $R_{bq}^{\text{pert}}$  to  $R_{bd}^{\text{pert}}$  for which the perturbative calculations have been performed.

The general form of the NLO prediction for  $R_{bd}^{\text{pert}}$  as a function of the running  $b$ -quark mass  $m_b$  is of the form

$$R_{bd}^{\text{pert}} = 1 + \frac{m_b^2}{M_Z^2} \left[ b_0(m_b) + \frac{\alpha_s}{2\pi} b_1(m_b) \right]. \quad (3)$$

The ratio can also be expressed in terms of the pole mass  $M_b$

$$R_{bd}^{\text{pert}} = 1 + \frac{M_b^2}{M_Z^2} \left[ b_0^P(M_b) + \frac{\alpha_s}{2\pi} b_1^P(M_b) \right]. \quad (4)$$

The two predictions are equivalent at this order. The coefficient functions  $b_{0,1}$  for the two

schemes can be related to each other by expressing the pole mass in terms of the running mass

$$M_b = m_b(\mu) \left[ 1 + \frac{\alpha_s(\mu)}{2\pi} \left( \frac{4}{3} - 2 \ln \frac{m_b(\mu)^2}{\mu^2} \right) \right]. \quad (5)$$

The coefficient functions  $b_0$  and  $b_1$  have been computed for the ratio of three and four jet rates [3,11]. The three jet rate ratio allows a NLO prediction, while for the four jet rate only a LO prediction is available. For the other variables used by ALEPH the predictions have been obtained using the MC generators ZBB4[11] and EVENT[12] which are correct to NLO. The hadronization corrections have been evaluated for all variables by computing the relevant observables at parton and at hadron level.

### 3. ALEPH analysis

In the ALEPH analysis data taken at the peak of the  $Z$  resonance from 1991 to 1995 are used. A standard hadronic event selection [8] is applied, which is based on charged particles. A cut  $|\cos \theta_T| < 0.7$  is imposed, where  $\theta_T$  is the polar angle of the thrust axis, computed from all charged and neutral particles as obtained from the energy-flow algorithm [14]. This requirement ensures that the events are well contained within the vertex detector (VDET) acceptance. After the selection, a sample of 2.3 million hadronic events remains for further analysis, with about 0.3% of non-hadronic background, mainly coming from  $\tau^+\tau^-$  events.

An important ingredient of the analysis is the choice of the Monte Carlo simulation, which is based on on JETSET 7.4 parton shower model plus string fragmentation [15]. The production rates, decay modes and lifetimes of heavy hadrons are adjusted to agree with recent measurements, while heavy quarks are fragmented using the Peterson et al. model [16].

The observables described in Section 2 are computed using only charged tracks.

In the analysis only  $b$  events are tagged. The selection is based on the long  $b$  hadron lifetime thanks to the great precision of the VDET, and follows closely the approach described in detail in Ref. [17]. The actual selection of  $b$  events is

Table 1

Leading (LO) and next-to-leading (NLO) order contributions to  $1 - R_{bd}^{\text{pert}}$ , for the running mass (run) and the pole mass (pol) schemes. The contributions are evaluated for a running (pole) mass of 3 (5)  $\text{GeV}/c^2$ . The strong coupling  $\alpha_s(M_Z)$  is set to 0.119. The values are given for the three-jet rate (DURHAM scheme) and for the event-shape variables thrust  $T$ ,  $C$  parameter, the transition value  $y_3$  for three to two jets (DURHAM scheme), and the total and wide jet broadenings ( $B_T$  and  $B_W$ ). The indices indicate the first or second moment of the event shape variable.

$O$	run		pol	
	LO	NLO	LO	NLO
$R_3$	0.020	0.010	0.056	-0.008
$T_1$	0.036	0.019	0.076	-0.007
$T_2$	0.017	0.032	0.043	0.036
$C_1$	0.044	0.022	0.091	-0.011
$C_2$	0.021	0.039	0.052	0.043
$y_{3_1}$	0.032	0.007	0.071	-0.021
$y_{3_2}$	0.015	0.003	0.032	-0.007
$B_{T_1}$	0.117	0.006	0.188	-0.074
$B_{T_2}$	0.036	0.112	0.080	0.123
$B_{W_1}$	0.117	-0.085	0.188	-0.183
$B_{W_2}$	0.036	0.016	0.080	-0.013

obtained from a cut on the distribution of the confidence level  $P_{uds}$  that all tracks of the event come from the main vertex. Very good agreement between data and MC is observed. On  $b$  events the selection has an efficiency of 80.5% and a purity of  $\mathcal{P}_{bb} = 83.1\%$ . The backgrounds amount to  $\mathcal{P}_{bc} = 13.5\%$  and  $\mathcal{P}_{bq} = 3.4\%$ .

### 3.1. Choice of variables

A list of the leading (LO) and next-to-leading order (NLO) contributions to  $1 - R_{bd}^{\text{pert}}$  is given in Table 1 for all variables, both for the running and the pole mass schemes. They have been evaluated for a  $b$ -quark mass of 3  $\text{GeV}/c^2$  in the former and 5  $\text{GeV}/c^2$  in the latter case. It is found that for some observables such as the jet broadening variables the mass effect is rather large. However, the NLO corrections can also be sizeable, as in the case of the second moment of thrust and the first moment of the wide jet broadening. For such variables it would definitely be necessary to also compute the NNLO contributions in order to obtain a

reliable perturbative prediction. Because of these observations only those variables are considered for which in both schemes the NLO contribution is clearly smaller than the LO term.

### 3.2. Hadronization corrections

The perturbative predictions are corrected for hadronization effects by computing the relevant observables at parton and at hadron level, including final state photon radiation off quarks. Several Monte Carlo models based on the parton shower approach plus subsequent string or cluster fragmentation are employed for this purpose. For the nominal analysis, the same generator as for the full simulation is used.

The ratios of hadronization corrections,  $H_{b/q}$ , are listed in Table 2. The corrections are rather sizeable for almost all the observables; in most cases they are of the same size as or larger than the expected mass effect. Only the three-jet rate and the first two moments of the  $y_3$  distribution have corrections at the 2% level or below. For

all the other event-shape variables the corrections are of the order of 10% or even larger. It has been found that the deviation from unity is almost entirely due to  $b$  hadron decays, which change the distributions mainly in the two-jet region. As can be observed from Table 2, the same corrections, computed taking only hadrons which stem directly from the string before any decay, come close to unity within one or two percent. This is in agreement with expectations from recent calculations of nonperturbative power-law corrections to moments of event-shape distributions for massive quarks [18].

By requiring that the hadronization corrections do not exceed 2% two variables remain: the first moment of  $y_3$  and the three jet ratio.

### 3.3. Measurement of $R_{bd}^{\text{pert}}$

The results for the perturbative ratio  $R_{bd}^{\text{pert}}$  are listed in Table 2, after having applied the correction procedure defined in equation 2 and correcting for anomalous triangle diagrams.

The dependence on the resolution parameter  $y_{\text{cut}}$  of the perturbative ratio  $R_{bd}^{\text{pert}}$  for the three-jet rate is indicated in Fig. 1.

The data are compared to the predictions of the parton shower models of PYTHIA 6.1, which is based on JETSET, and HERWIG 6.1 [19]. The MC models are in reasonable agreement with the measurement at large  $y_{\text{cut}}$  values, where the statistical uncertainty is large, however. At intermediate resolution parameters these models predict a lower ratio than observed.

In addition, in Fig. 1 the next-to-leading order perturbative QCD predictions for two different values of the running  $b$ -quark mass in the  $\overline{\text{MS}}$  scheme are given. The data clearly favour a mass close to  $3 \text{ GeV}/c^2$ .

### 3.4. Systematic errors

Systematic uncertainties on the mass extraction can be divided into three categories: the ones coming from uncertainties on the tagging biases, from the hadronization and from the missing higher order corrections.

The first ones have been evaluated by varying the gluon splitting rate which influences the purity of the  $b$  tag and by studying the variation of

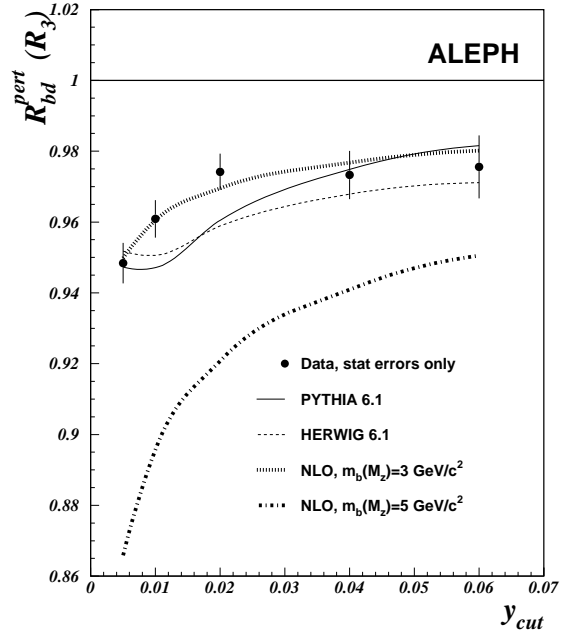


Figure 1. Comparison of the  $y_{\text{cut}}$  dependence of the measured ratio  $R_{bd}^{\text{pert}}$  for the three-jet rate to the predictions of parton shower models as well as next-to-leading order (NLO) perturbative QCD for two different values of the  $b$ -quark mass in the  $\overline{\text{MS}}$  scheme. The errors are statistical only.

the results due to the inadequacy of the simulation of the tracking detectors.

The uncertainties from the modelling of the hadronization are typically evaluated by computing the hadronization corrections with different MC generators. As has been shown in Section 3.2, the  $b$  hadron decays have a large impact on the size of the hadronization corrections. Because in the tuning of the MC hadronic final states are analyzed after all decays, differences in the description of hadron decays can lead to differences in the tuned fragmentation parameters. In order to assess an uncertainty related to the string fragmentation parameters and subsequent decays, the

Table 2

ALEPH results for  $R_{bd}^{\text{pert}}$  with statistical errors, including the uncertainty from the MC statistics. The results are obtained with the hadronization corrections  $H_{b/q}$  as predicted by the MC. Also given are the corrections  $H_{b/q}^{\text{nod}}$ , computed from hadrons directly originating from the string, before any decays (*nod*=no decays).

$O$	$R_{bd}^{\text{pert}}$	$H_{b/q}$	$H_{b/q}^{\text{nod}}$
$R_3$	$0.974 \pm 0.005$	0.980	0.987
$T_1$	$0.910 \pm 0.002$	1.134	1.003
$C_1$	$0.894 \pm 0.002$	1.169	1.009
$y_{31}$	$0.955 \pm 0.005$	1.023	0.987
$y_{32}$	$0.979 \pm 0.010$	0.984	0.984
$B_{T_1}$	$0.831 \pm 0.001$	1.306	1.025
$B_{W_2}$	$0.929 \pm 0.003$	1.088	0.986

variation in the final result when using two different  $b$  hadron decay tables for the hadronization corrections is taken as a systematic uncertainty.

Another quantity relevant for this analysis is the  $b$  fragmentation function, which describes the energy fraction transferred to the  $b$  hadrons during the fragmentation process. Three different sets of different fragmentation functions were used to assess the systematic uncertainty due to this source. Finally, in order to study purely the difference between string and cluster fragmentation, the variation in the hadronization corrections for light quarks ( $uds$ ) only has been propagated into an uncertainty on the final result.

Missing higher order corrections are estimated by extracting firstly the pole mass from the perturbative expression in the pole mass scheme, then translating that result into a running quark mass  $m_b(m_b)$  at the  $b$ -mass scale, and finally running this mass up to the  $M_Z$  scale using the renormalization group equation. In addition, the effects of uncalculated higher order terms can be estimated by a change in the renormalization scale. For the central value  $\mu = M_Z$  is employed, and the systematic error is taken to be half of the range of mass values (average of running and pole mass schemes) found when varying  $\mu$  from  $0.1M_Z$  to  $2M_Z$ . The behaviour of the extracted mass in the two schemes as a function of the renormalization scale  $\mu$  is illustrated in Fig. 2 for the first

moment of the  $y_3$  variable.

### 3.5. Results for $m_b(M_Z)$

Based on the predictions obtained above, the running  $b$ -quark mass is determined from the measured ratio  $R_{bd}^{\text{pert}}$  for two observables, the first moment of the  $y_3$  distribution and the three-jet rate.

As stated in Section 2, the functional dependence of the coefficients  $b_{0,1}$  for the moments of the event shape variables are computed by the ratio of the cross sections for  $b$  and  $d$  quarks using the MC generators ZBB4 [11] and EVENT [12]. ZBB4 allows for the integration of the fully differential NLO matrix elements including mass effects, whereas EVENT contains the massless expressions [13].

In Fig. 3 an example of these fits is shown for the first moment of the  $y_3$  distribution. With these parametrisations it is possible to estimate the actual quark mass effects in leading order and its next-to-leading order corrections. In Table 1 a list of these LO and NLO contributions is given for all variables for both the running and the pole mass schemes.

The results are listed in Table 3 together with the statistical and systematic uncertainties, which have been propagated from the corresponding uncertainties on  $R_{bd}^{\text{pert}}$ . The result from the first moment of the  $y_3$  observable is quoted as

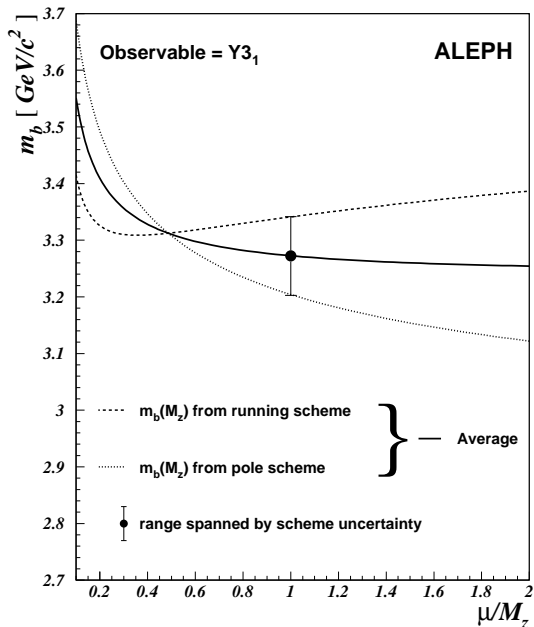


Figure 2. Renormalization scale dependence for the extracted  $b$ -quark mass in the running and pole mass scheme, for the observable  $y_{3,1}$ . The error bar spans the range of the scheme uncertainty. The full line indicates the renormalization scale dependence of the average computed from the running and pole mass schemes.

the final  $b$ -quark mass value, due to its smaller hadronization and systematics errors. The theoretical uncertainty is estimated as described in Section 3.4 by evaluating the impact of the uncertainty on the strong coupling constant and the renormalization scale variation. Because the pole and the running mass scheme are equivalent at NLO, the average of the values found for the two schemes is quoted as the final result, and half of the difference is taken as an additional theoretical systematic uncertainty due to the scheme ambiguity. This leads to a measurement of the  $b$ -quark

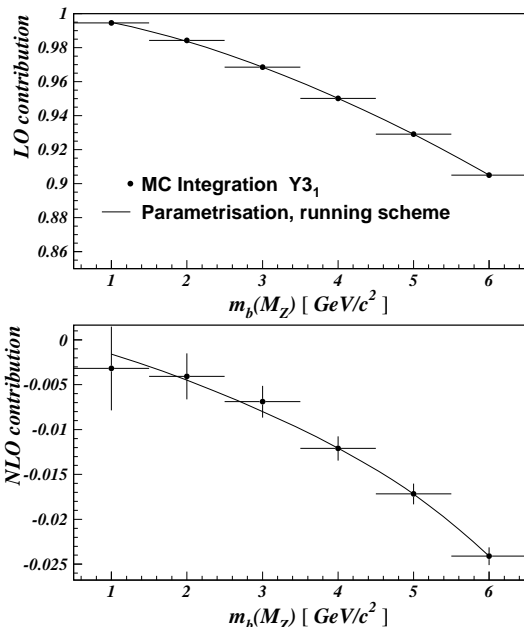


Figure 3. Parametrisations of the  $b$ -quark mass dependence for the LO (top) and NLO (bottom) contributions to  $R_{bd}^{\text{pert}}$  in the running mass scheme for the first moment of the  $y_3$  distribution. The points indicate the result of the MC integration, and the full line the parametrisations. The NLO contributions are evaluated using  $\alpha_s(M_Z) = 0.119$ .

mass from ALEPH of

$$m_b(M_Z) = [3.27 \pm 0.22(\text{stat}) \pm 0.22(\text{exp}) \pm 0.38(\text{had}) \pm 0.16(\text{theo})] \text{ GeV}/c^2. \quad (6)$$

#### 4. DELPHI analysis

The first measurement of the running  $b$ -quark mass at scales of the  $Z$  mass has been performed by DELPHI, using 1992 to 1994 data and the three jet rate ratio using the Durham algorithm for jet clustering [5]. Effects of the running of the  $b$ -quark mass have also been measured in the four

Table 3

ALEPH measured  $b$ -quark mass  $m_b(M_Z)$  in the  $\overline{\text{MS}}$  scheme with statistical (stat), experimental (exp) and hadronization (had) uncertainties. In the last column the measured pole mass  $M_b$  is listed.

$O$	$m_b(M_Z)$ [GeV/ $c^2$ ]	$\pm(\text{stat})$	$\pm(\text{exp})$	$\pm(\text{had})$	$M_b$ [GeV/ $c^2$ ]
$R_3$	2.76	0.28	0.28	0.62	3.65
$y_{3_1}$	3.34	0.22	0.22	0.38	4.73

jet rate ratio as reported in [20].

A new analysis has been presented at this conference which is based on the 1994 and 1995 data sample, which amounts to about 1.3 Million hadronic  $Z$  decays. A better  $b$  tagging algorithm was developed, which is described in [22]. The efficiency to tag  $b$  events is about 53% with a 85% purity.

The Monte Carlo model used is based on PYTHIA, with the DELPHI tuning.

The study was performed using the DURHAM and CAMBRIDGE[21] jet algorithms. The latter is found to minimize the NLO corrections to the three jet rate for the running  $b$ -quark mass [21].

#### 4.1. Measurement of $R_{bd}^{\text{pert}}$

The three jet ratio is shown in Figure 4 for both jet algorithms. As can be seen the LO calculation did not provide good description of the data and NLO corrections are indeed needed. In the case of DURHAM the data are closer to the running  $b$ -quark mass calculations, despite the NLO corrections are larger with respect to the pole mass. For the CAMBRIDGE algorithm data still prefer the running  $b$ -quark mass calculations, but here the NLO corrections are in fact smaller for this scheme.

#### 4.2. Systematic errors

Hadronization errors were derived from comparisons with different Monte Carlo models tuned to describe the data. Two different sources of errors were considered:  $\sigma_{\text{mod}}$  which describes the difference of the hadronization corrections between PYTHIA and HERWIG, and  $\sigma_{\text{tun}}$  which accounts for the possible variation of the main fragmentation parameters in PYTHIA. The first uncertainty takes into account both the different fragmentation scheme (string or cluster) and the dif-

ferent  $b$  hadron decay tables. In the case of  $\sigma_{\text{tun}}$  the error was evaluated by changing the most relevant fragmentation parameters of the string model in PYTHIA by  $\pm 2\sigma$  from their central tuned values and assuming they are uncorrelated. The two above errors were combined in quadrature to estimate the hadronization uncertainty. The interval of validity for the jet resolution parameter  $y_{\text{cut}}$  to perform the measurement was chosen to have small hadronization error (below 5%) and smooth  $y_{\text{cut}}$  dependence. Figure 5 shows the total hadronization correction uncertainty for the three jet rate for the two jet algorithms.

The uncertainty coming from the tagging is taken into account by varying the purities by 1%.

The errors coming from missing higher orders are estimated by varying the renormalization scale  $\mu = M_Z$  from 0.5 to 2. The ambiguity due to the definition of the three jet rate in terms of the running or the pole  $b$ -quark mass has been evaluated as explained in Section 3.4.

#### 4.3. Extraction of the $b$ -quark mass

The values for the running  $b$ -quark mass obtained with the DURHAM and CAMBRIDGE algorithms are shown in Table 4, for  $y_{\text{cut}} = 0.02$  and 0.005, respectively.

The three jet rate measured with the CAMBRIDGE algorithm is in agreement with both LO and NLO calculations in terms of the running  $b$ -quark mass. For this reason the mass is extracted from this algorithm using the NLO prediction. The value of the running  $b$ -quark mass from DELPHI is therefore

$$m_b(M_Z) = [2.61 \pm 0.18(\text{stat})_{-0.49}^{+0.45}(\text{frag.}) \pm 0.18(\text{tag.}) \pm 0.07(\text{theo.})] \text{ GeV}/c^2. \quad (7)$$

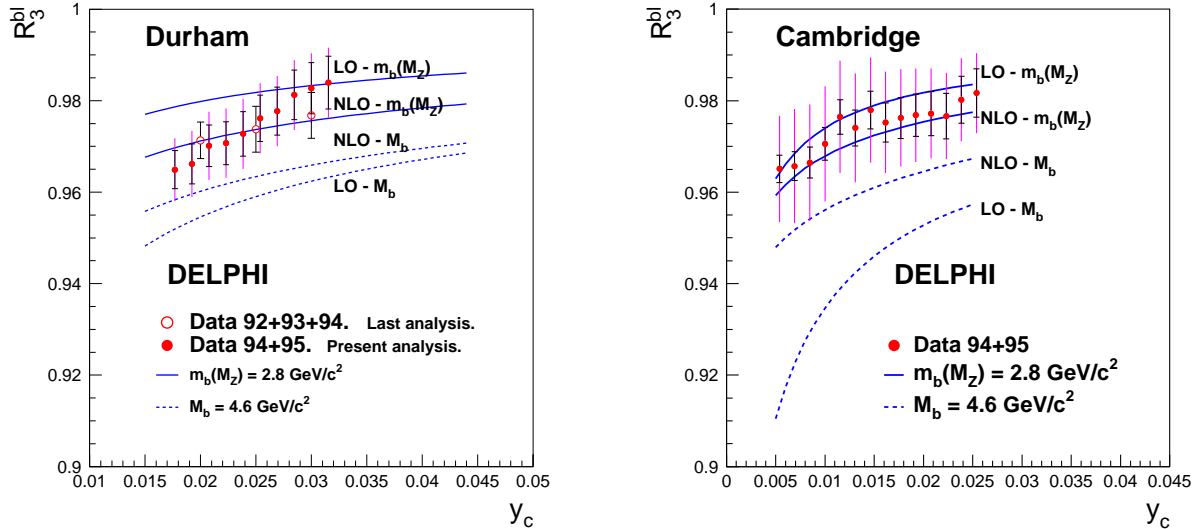


Figure 4. Corrected data values of the perturbative three jet ratio using DURHAM (left) and CAMBRIDGE (right) jet algorithms for DELPHI, compared with the theoretical predictions from [3] at LO and NLO in terms of the pole mass  $M_b = 4.6 \text{ GeV}/c^2$  (dashed lines) and in terms of the running mass  $m_b(M_Z) = 2.8 \text{ GeV}/c^2$  (solid lines).

## 5. Conclusions

ALEPH has studied a large set of observables to extract the  $b$ -quark mass at the  $Z$  peak. The first moment of  $y_3$  has the smallest hadronization and systematic errors. DELPHI used instead the three jet ratio using the CAMBRIDGE jet algorithm which is found to minimize the NLO corrections for the running  $b$ -quark mass.

Clear effects due to the running of the  $b$ -quark mass are visible and confirm the expectation from QCD. The results from ALEPH, DELPHI and a measurement from Brandenburg *et al.* [23] are shown in Fig. 6, together with the average of the low energy measurements for  $m_b(m_b)$  [24], which is evolved up to the  $Z$  mass scale using a two-loop evolution equation with  $\alpha_s = 0.119 \pm 0.003$ .

The main error on the measurement comes from the uncertainties affecting the hadronization corrections. A big fraction of it is coming from

$b$  hadron decays as has been estimated in great detail by ALEPH.

Despite of the fact that the  $b$ -quark mass measured from the three jet ratio from ALEPH and DELPHI shows a good agreement.

The mass extracted from the first moment of  $y_3$  seems to be larger and barely compatible with the jet ratio measurements.

The spread in the central value and the actual size of the errors indicate that the limiting precision of the measurement of the  $b$ -quark mass at the  $Z$  mass scale is of the order of  $500 \text{ MeV}/c^2$ .

## 6. Acknowledgements

I would like to thank Prof. Narison for ruling the Conference in a nicely informal atmosphere. I am also grateful J. Fuster, S. Martí i García and G. Dissertori for useful discussions.



Table 4

DELPHI measured  $b$ -quark mass  $m_b(M_Z)$  in the  $\overline{\text{MS}}$  scheme with statistical (stat), hadronization (frag.),  $b$  tagging (b-tag) and theoretical (theo) uncertainties. The first line contains the results of the previous published analysis.

$y_{cut}$	Algorithm	$m_b(M_Z)$ [GeV/ $c^2$ ]	$\pm(\text{stat})$	$\pm(\text{frag})$	$\pm(\text{b-tag})$	$\pm(\text{theo})$	Data
0.02	DURHAM	2.67	0.25	0.34	-	0.27	[5]
0.02	DURHAM	2.81	0.25	0.34	0.20	0.27	[6]
0.005	CAMBRIDGE	2.61	0.18	$^{+0.45}_{-0.49}$	0.18	0.07	[6]

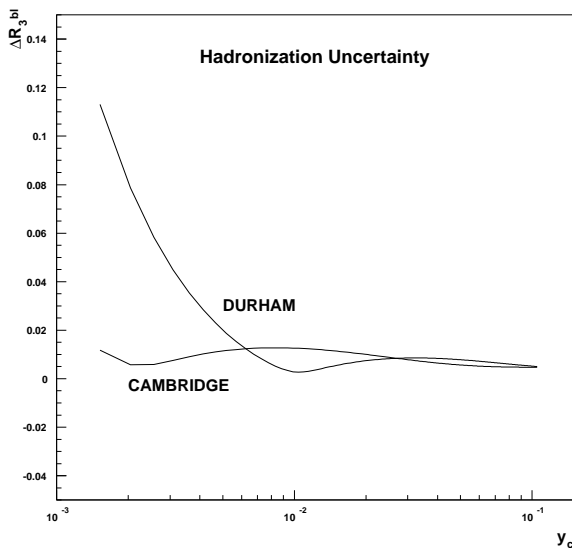


Figure 5. Evolution of the total hadronization error on the three jet ratio for the DELPHI analysis with the resolution parameter  $y_c$ . The error corresponds to two times the sum in quadrature of  $\sigma_{\text{tun}}$  and  $\sigma_{\text{mod}}$ , as described in the text.

## REFERENCES

1. S. Narison, Phys. Lett. **B352** (1995) 122.  
M. Jamin and A. Pich, Nucl. Phys. **B507** (1997) 304.
2. V. Gimenez, L. Giusti, G. Martinelli and F. Rapuano, hep-lat/0002007, February 2000.
3. G. Rodrigo, QCD96 Montpellier, hep-ph/9609213 and Nucl. Phys. Proc. Suppl. **54A** (1997) 60.  
G. Rodrigo, M. Bilenky, A. Santamaria, Phys. Rev. Lett. **79** (1997) 193.
4. The ALEPH Collab., CERN EP/2000-093 (Submitted to European Physical Journal C)
5. The DELPHI Collab., Phys. Lett. **B418** (1998) 430.
6. The DELPHI Collab., DELPHI Conference paper 420, 4 July, 2000.
7. S. Catani et al., Phys. Lett. **B269** (1991) 179; N. Brown and J. Stirling, Z. Phys. **C53** (1992) 629.
8. ALEPH Collab., Phys. Rep. **294** (1998) 1.
9. S. Catani, G. Turnock, and B.R. Webber, Phys. Lett. **B295** (1992) 269.
10. K. Hagiwara, T. Kuruma, and Y. Yamada, Nucl. Phys. **B358** (1991) 80;
11. P. Nason, C. Oleari, Phys. Lett. **B407** (1997) 57.
12. G. Altarelli, R. Kleiss, C. Verzegnassi, *Z Physics at LEP1*, CERN Yellow Report 89-08, vol.1, p.373.
13. R.K. Ellis, D.A. Ross, A.E. Terrano, Nucl. Phys. **B178** (1981) 421.
14. The ALEPH Collab., Nucl. Instr. Meth. **A360** (1995) 481.
15. T. Sjöstrand, Comp. Phys. Comm. **82** (1994) 74.
16. C. Peterson et al., Phys. Rev. **D27** (1983) 105.
17. The ALEPH Collab., Phys. Lett. **B313** (1993) 535.
18. Z. Trocsanyi, JHEP **0001** (2000) 014.
19. G. Marchesini et al., Comp. Phys. Comm. **67** (1992) 465.
20. The DELPHI Collab., Contributed paper No.

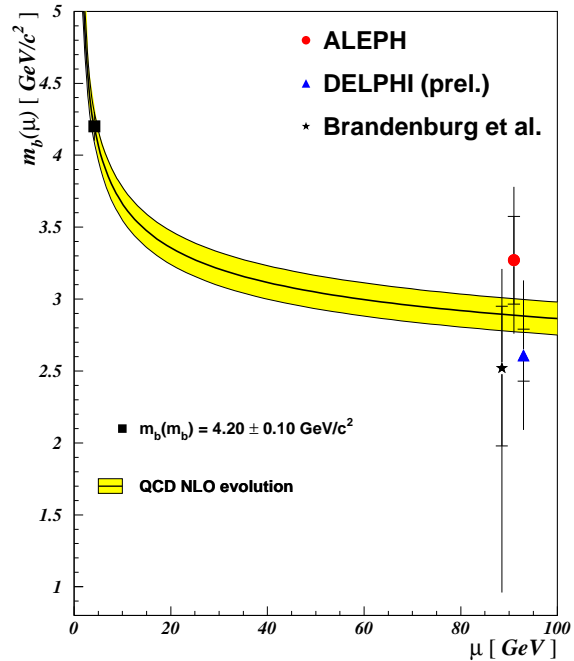


Figure 6. Comparison of the ALEPH and DELPHI result for  $m_b(M_Z)$  with the world average value of low-energy measurements for  $m_b(m_b)$  [24], which is evolved up to the  $M_Z$  scale using a two-loop evolution equation with  $\alpha_s(M_Z) = 0.119 \pm 0.003$ . Also shown is the measurements by Brandenburg et al. [23]. The inner error bars indicate the quadratic sum of the statistical and experimental uncertainties. The three points at the Z pole are separated for clarity.

- 1\_223 to the HEP'99 Conference, Tampere, Finland, DELPHI 99-121 CONF 308.
21. Yu.L. Dokshitzer, G.D. Leder, S. Moretti and B.R. Webber, J. High Energy Phys. **08:001**, 1997.
  22. The DELPHI Collab., Eur. Phys. J. **C 10**, (1999) 415.
  23. A. Brandenburg et al., Phys. Lett. **B468** (1999) 168.
  24. A. Pich, hep-ph/000118, January 2000.